An antisense oligonucleotide leads to suppressed transcriptional elongation of *Hdac2* and long-term memory enhancement

Celeste B. Greer[1†], Shane G. Poplawski[2,3†], Krassimira A. Garbett[1], Rebekah L. McMahan[1], Holly B. Kordasiewicz[4], Hien Zhao[4], Andrew J. Kennedy[6], Slavina B. Goleva[5], Teresa H. Sanders[1], S. Timothy Motley[3], Eric E. Swayze[4], David J. Ecker[3], Todd P. Michael[2,3*], and J. David Sweatt[1*]

Affiliations:

[1]Department of Pharmacology, Vanderbilt University, Nashville, TN, USA

[2]J. Craig Venter Institute, CA, USA

[3]Ibis Biosciences an Abbott Company, Carlsbad, CA, USA

[4]Ionis Pharmaceuticals, Carlsbad, CA, USA

[5]Department of Molecular Physiology and Biophysics, Vanderbilt University, Nashville, TN, USA

[6]Department of Chemistry, Bates College, Lewiston, ME, USA

†Co-first authors

*Co-corresponding authors

Correspondence:

J. David Sweatt, Ph.D.

Professor and Chairman

Vanderbilt University

Department of Pharmacology

2220 Pierce Avenue, 476 RRB

Nashville, TN 37232

Phone: 615-343-3533

david.sweatt@vanderbilt.edu

Todd P. Michael, Ph.D.

Professor and Director of Informatics

J. Craig Venter Institute

4120 Capricorn Ln.

La Jolla, CA 92037

Phone: 858-200-1864

tmichael@jcvi.org

ABSTRACT

The memory suppressor gene histone deacetylase 2 (*Hdac2*) is a target of small molecule inhibitors under investigation for their effects on cognitive enhancement and treating disorders of memory. The therapeutic compounds currently available are not completely specific to the *Hdac2* isoform, and have short half-lives. Antisense oligonucleotides (ASOs) are FDA-approved to treat several diseases. They are a class of drugs that base pair with their target RNA and their effects are extremely long lasting compared to small molecule inhibitors. We utilized an ASO to specifically reduce *Hdac2* messenger RNA (mRNA) quantities. We explored the longevity and mechanism of mRNA repression of our *Hdac2* specific ASO. A single dose of the *Hdac2*-targeted ASO injected into the central nervous system diminished *Hdac2* mRNA levels for at least 4 months in the brain, and knockdown of this factor resulted in significant memory enhancement. RNA-seq analysis of brain tissues revealed that reducing *Hdac2* mRNA with the ASO caused alteration of steady-state levels for other memory-associated mRNAs. In looking at target knockdown in cultured neurons, we observed that our *Hdac2*-targeted ASO suppresses *Hdac2* mRNA as well as an *Hdac2* non-coding RNA. Importantly, we found that the ASO not only triggered a reduction in mRNA levels, but also elicited a direct transcriptional suppression of the *Hdac2* gene by blocking RNA polymerase II elongation. These findings suggest transcriptional suppression of the target gene as a potential novel mechanism of action of ASOs, and opens up the possibility of using ASOs to achieve lasting gene silencing in without altering the nucleotide sequence of a gene.

INTRODUCTION

Long-term memory formation and retention requires coordinated transcriptional changes, and evidence implicates the epigenome in this process. Decreasing acetylation by inhibiting histone acetyltransferases (HATs) such as CREB-binding protein (CBP) impairs long-term memory [1-3], while increasing acetylation by inhibiting histone deacetylases (HDACs) enhances long-term memory [4,5]. Eleven isoforms of classical HDAC proteins exist in mammals, and evidence suggests HDAC2 in particular is responsible for regulating synaptic plasticity and memory formation relative to its close homolog HDAC1 and other HDAC isoforms [6]. Translating this knowledge therapeutically has been difficult because many small molecule HDAC inhibitors are hampered by poor pharmacokinetics and promiscuous subtype selectivity.

Antisense oligonucleotide (ASO) therapies utilize base pairing with a target messenger RNA (mRNA) to achieve selectivity, so we were interested in designing and testing an ASO targeting *Hdac2* mRNA. Our prior work shows that the *Hdac2* ASO elicited substantial memory enhancement in wild-type mice in object location memory tests, and it rescued impaired performance in fear conditioning and Morris water maze tasks in a mouse model of autism [7]. ASOs targeting other mRNAs can reduce expression of genes in the central nervous system (CNS) [8], and the knockdown persists for months after the last delivery of the drug [9,10]. ASOs are FDA-approved for treatment of several diseases [11], and are in clinical trials for Huntington's disease [12].

The two most commonly utilized mechanisms of action for ASOs in therapeutic applications are 1) recruitment of RNaseH1 to the RNA/ASO hybrid and subsequent degradation of the RNA [13], and 2) correction of splicing defects that lead to disease when the ASO is designed to target splice junctions [14,15]. Because ASOs can modulate splicing, which occurs during the transcription of RNA [16-19], we reasoned ASOs could possibly interfere with transcription itself. Therefore, we examined more closely whether ASOs only mediate RNA degradation or might also be involved in preventing their transcriptional synthesis.

We report here that the *Hdac2*-targeting ASO is specific, long lasting, and blocks *Hdac2* transcription. A single injection of *Hdac2*-targeted ASO in vivo reduced *Hdac2* mRNA for at least 4 months, and increased memory for 8 weeks. Furthermore, it affects the expression levels of hundreds of genes in the brain. These genes are involved in extracellular signal-regulated kinase (ERK) signaling, memory-associated "immune" functions, synapse formation, and the regulation of flavonoids. Although the *Hdac2* ASO used herein was designed to mediate degradation of target mRNA, we also found that the ASO elicits transcriptional suppression of its target gene by blocking RNA polymerase II (RNA Pol II) elongation.

RESULTS

Hdac2-targeted ASOs and validation of isoform specificity

For our studies, we chose *Hdac2*-targeting ASOs that can achieve potent knockdown [7]. We predominantly utilized *Hdac2* ASO1, but *Hdac2* ASO2 was used to see if our mechanistic findings are specific to ASO1 or generalizable to another ASO targeting *Hdac2* RNA at a different site. ASO1 targets the 3' untranslated region (UTR), and ASO2 targets exon 10 (Fig. 1a). A structurally similar scrambled (SCR) control ASO that targets no known mouse genes was used as a control.

We used reverse transcription followed by quantitative PCR (RT-qPCR) to show that our *Hdac2* ASOs knockdown *Hdac2* mRNA in mouse primary cortical neurons after a week of treatment relative to controls (Fig. 1b). Furthermore, the two *Hdac2* ASOs show no suppression of closely related *Hdac1* mRNA (Fig. 1c), demonstrating its isoform specificity. *Hdac1* actually showed slightly increased RNA expression, which may be indicative of a compensatory mechanism [20]. We confirmed the efficacy and specificity of the ASOs in a mouse neuroblastoma Neuro2a (N2a) cell line differentiated with serum-starvation conditions (dN2a, Fig. S1a), since this culture system was also used in some of our later experiments. The *Hdac2* ASOs again repress *Hdac2* (Fig. S1a), but not *Hdac1* mRNA (Fig. S1c).

Phosphorothiate and 2´-MOE modified ASOs have been shown to elicit selective and prolonged RNA knockdown in the brain [10,21,22]. Therefore, we wanted to see if *Hdac2* ASO1 elicits persistent repression of *Hdac2* mRNA. Using primary neurons, we found that 14 days after rinsing and washing out the targeting ASO, *Hdac2* mRNA levels were still significantly reduced (Fig. 1d). ASO-mediated repression of *Hdac2* mRNA expression is persistent in cell culture.

Long-term target knockdown and behavioral memory enhancement in vivo

Because of the persistence in vitro, we next wanted to test the longevity of *Hdac2* ASO1 action in the brain. We did a single intracerebroventricular (ICV) injection of *Hdac2* ASO1 in mice, and examined molecular and behavioral changes out to 40 weeks post-surgery. The targeting ASO significantly reduces *Hdac2* mRNA in the cortex for 32 weeks after a single *Hdac2* ASO1 injection (Fig. 2a). HDAC2 protein was significantly lower in the *Hdac2* ASO1 group compared to the scrambled group in cortex from 3 days to 16 weeks after treatment (Fig. 2b). ICV injection also elicits repression of *Hdac2* RNA level in the hippocampus (Fig. 2c). Although ASO1 targets the 3' UTR of the *Hdac2* gene, all exons exhibited a similar level of reduction at each exon in our sequencing data (Fig. S2a). HDAC2 protein expression is also reduced 2, 8, and 16 weeks after injection in the hippocampus (Fig. 2d). The liver, which is one of the primary peripheral sites of ASO accumulation [23], showed no significant mRNA or protein reduction at the two time points tested (2 and 32 weeks) after ICV injection (Fig. S2b). Perhaps because of its anatomical distance from the cerebral ventricles, the cerebellum revealed milder knockdown. Significant repression occurred between 2 and 16 weeks after ICV, but knockdown was greater than 50% of *Hdac2* mRNA level compared to SCR ASO treated mice. Protein analysis showed no significant repression of protein levels at 2 and 32 weeks (Fig. S2c).

Blocking HDAC2 has been shown to enhance memory formation, so we tested the duration of spatial memory enhancement in the ICV-injected mice. We used an object location memory (OLM) assessment of the treated animals at weeks 2, 8 and 16. Briefly, the OLM assessment is based on the spontaneous tendency of rodents to spend more time exploring an object that has been relocated. A

higher discrimination index indicates that the mouse remembers the familiar placement. Animals that received a single ICV injection of *Hdac2* ASO1 had a higher discrimination index compared to mice that received the control SCR ASO, with statistically significant effects at weeks 2 and 8 and a trend at 16 weeks (Fig. 2e).

Hdac2 ASO1 does not cross the brood-brain barrier

Previous reports show that ASOs do not cross the blood-brain barrier [24,25], and we wanted to know if this was true for *Hdac2* ASOs. Consistent with prior studies, injection of *Hdac2* ASO1 into the tail vein did not repress *Hdac2* mRNA in the brain. However, we do see knockdown in the liver at 2 weeks in these animals (Fig. S2d).

Global transcription changes induced by *Hdac2* ASO1

Because HDAC2 is a regulator of histone acetylation, chronic reduction of HDAC2 protein is expected to cause changes to the transcriptome. RNA-seq of mice during 2 to 8 weeks, when animals had significantly enhanced memory in OLM (Fig. 2e), showed significant changes in many genes. In both the cortex and hippocampus, *Hdac2* ASO1 significantly altered the expression of genes with immune functions and genes with involvement in ERK signaling. Although some of the genes identified were first identified in the immune system, many of these genes also have known roles in memory (38). Other subgroups of genes that are identified in the cortex (Fig. 3a, blue cluster and red cluster, Table S2) are involved in cell adhesion, transcription, neuron projections, synapse organization, and myelination. The red cluster in Fig. 3b, represents a set of genes that are significantly changed in the hippocampus (Table S3). The genes in this group are involved in glucuronidation and flavonoid biosynthesis.

ASO regulation of a putative *Hdac2* extra-coding RNA

Previous work has demonstrated the existence of extra-coding RNAs (ecRNA) generated from many neuronal genes, which promote their transcription [26,27]. These RNAs are sense transcripts that are unspliced and transcribe over mRNA sequences and prevent repression of their gene of origin. ecRNAs begin transcription upstream of the transcription start site (TSS), and terminate downstream of the transcription end site (TES) of the gene they regulate. Since ecRNAs contain all of the sequences within the mRNA they control, our *Hdac2* mRNA-targeting ASOs have target sequences matching both mRNA and ecRNA. We know from previous work that *Fos* has an ecRNA regulating its expression, and targeting the ecRNA of *Fos* with an ASO designed against a region downstream of the TES of *Fos* can block *Fos* mRNA level [26]. We likewise found that *Fos* ecRNA ASOs block *Fos* mRNA transcript levels (Fig. S3a). Moreover, we found that a *Fos* mRNA-targeting ASO downregulates the expression of *Fos* ecRNA (Fig. S3b). This led us to investigate whether our *Hdac2* ASOs inhibit an *Hdac2* ecRNA.

We first looked for evidence that *Hdac2* has an ecRNA in previously published RNA-seq datasets from primary neuronal cultures of mice and rats. We used an RNA-seq library that detected lowly expressed and transient RNAs [28] and a dataset that identified ecRNAs in rat primary neurons. The second dataset has polyadenylated transcripts separated from non-polyadenylated transcripts to better identify the non-polyadenylated ecRNAs [26]. Both of the mentioned datasets show reads in regions upstream of the TSS, in introns, and extending beyond the 3'UTR of *Hdac2*, consistent with the presence of an *Hdac2* ecRNA (Fig. 4a). Furthermore, these *Hdac2* ecRNA reads are predominantly present in the non-polyadenylated fraction (Fig. 4a, PolyA- tracks). Looking at RNA from primary cortical neurons, we were able to detect signal at regions beyond the TES using RT-qPCR (Figure 4b), which should be unique to the ecRNA (shaded pink area Figure 4a). Furthermore, we found that treating the cells with *Hdac2* ASO1 or ASO2 reduces levels of transcripts beyond the TES relative to SCR ASO (Fig. 4b). Our *Hdac2*-targeting ASOs are capable of down-regulating the expression levels of the putative *Hdac2* ecRNA in addition to repressing *Hdac2* mRNA levels.

Hdac2 ASO causes no detectable change to DNA methylation at *Hdac2* gene

ecRNAs are reported to interact with DNA methyltransferases (DNMT), and prevent DNA methylation. If the ecRNA is eliminated, DNA methylation is increased and transcription of the gene the ecRNA regulates is reduced. Both DNMT1 and DNMT3a have been implicated in binding ecRNAs [26,27]. Contrary to prior models, we find that DNMT inhibitors 5-azacitidine (5-Aza) and RG108, which target both DNMT isoforms, do not antagonize the repression of *Hdac2* mRNA by *Hdac2* ASO1 even though they decrease *Hdac2* ecRNA expression (Fig. S3c). Furthermore, RG108 cannot overcome the suppression of *Fos* mRNA or *Fos* ecRNA that arises when cells are treated with an ASO targeting *Fos* ecRNA (Fig. S3d and 3e). Despite this, we tested for changes in DNMT3a binding across the *Hdac2* gene with ChIP-qPCR. There is a mild increase in DNMT3a binding 1.4 kilobases downstream of the *Hdac2* TES (Fig. S3f). Prior reports also showed that DNMTs interact in an area downstream of the TES of *Fos* [26]. Despite these binding changes, we do not observe alterations in DNA methylation after treatment with *Hdac2* ASO1 relative to SCR ASO measured by MeDIP-qPCR (Fig. S3g). In any case, a non-enzymatic function of DNMT3a could epigenetically alter transcriptional output [29].

Direct transcriptional suppression by ASOs

We tested the hypothesis that ASOs trigger transcriptional suppression of *Hdac2* mRNA production. To determine if ASO1 and ASO2 prevent *Hdac2* pre-mRNA production, we conducted NRO experiments to quantify nascent *Hdac2* transcripts. During NRO, newly synthesized transcripts are purified by immunoprecipitation (IP). The IP method we optimized was able to isolate BrU-labeled RNA (+ samples), while washing away unlabeled RNA (- samples) with very low background signal (Fig. 5a). The level of *Hdac2* pre-mRNA in the immunoprecipitated nascent RNA fraction was measured by RT-qPCR. We observed that *Hdac2* ASO1 treatment results in a significant reduction of transcription towards the 3' end of the *Hdac2* gene in the 3'UTR (Fig. 5b). *Hdac2* ASO2, although it targets a different exon, repressed *Hdac2* transcription in a similar pattern to ASO1 (Fig. S4a). Interestingly, transcription near the 5' end of the *Hdac2* gene was not impeded in the NRO assay in both cell culture

systems (Fig. 5b and Fig. S4a), which suggests that the elongation, but not the initiation, of transcription is blocked by the targeting ASO.

HDACs have been implicated in transcriptional suppression as well as activation [30,31], so we tested if the changes we observed in the NRO experiment were an indirect effect of blocking HDAC activity using two broad-spectrum HDAC inhibitors, sodium butyrate (NaBu) and Suberoylanilide Hydroxamic Acid (SAHA). There was no repression of *Hdac1* or *Hdac2* transcript levels (Fig. S4b), and *Hdac2* transcription in NRO assays were not blocked by NaBu (Fig. S4c). Treatment of the cells with SAHA also did not repress *Hdac2* transcript levels (Fig. S4d). Therefore, *Hdac2* ASOs directly reduce the transcription of their target gene irrespective of any epigenetic changes resulting from blocking deacetylation.

Based on the NRO assay, we predicted that RNA Pol II might be stalled near the promoter of the *Hdac2* gene, preventing production of full-length transcripts. Therefore, we tested if *Hdac2* mRNA expression is regulated by transcriptional pause release since not all genes are under the control of this mechanism of transcriptional regulation [31,32]. Positive transcription elongation factor b (P-TEFb) is an important regulator of transcriptional pausing, and it is inhibited by the small molecule inhibitor Flavopiridol (FLAVO) [33]. FLAVO inhibits *Hdac2* mRNA expression (Fig. 5c, Fig. S4e), so we conclude that RNA Pol II pausing is an important regulatory step in *Hdac2* mRNA expression levels. Next, we looked to see if RNA Pol II is stalled at the promoter after ASO treatment. The decrease in transcripts occurred downstream of *Hdac2* intron 1 in the NRO, so using ChIP-qPCR we looked for an accumulation of the initiated form of RNA Pol II, which is phosphorylated at serine 5 of the C-terminal domain repeat region (RNA Pol II-pS5) [34,35], at intron 1 of the *Hdac2* gene. We found more binding of this active form of RNA Pol II near the promoter of *Hdac2* (Fig. 5d).

We detected a reduction of the putative *Hdac2* ecRNA in total RNA in Fig. 4b, but we also wanted to know if ecRNA transcription was affected by *Hdac2* ASO treatment. Using NRO, we looked at ecRNA expression at 1.7 kilobase pairs (kbp) beyond the transcription end site, since this had the strongest repression of any site beyond the TES (Fig. 4b). The *Hdac2*-specific ASOs not only

repressed total ecRNA level, they also inhibited their synthesis (Fig. S4f). Based on this result, it is possible that the ASO initially leads to RNaseH1-dependent turnover of ecRNA, but eventually the transcriptional output of the ecRNA itself is also reduced.

DISCUSSION

Our studies indicate that nucleotide sequence-specific *Hdac2* ASOs provide a powerful avenue for targeting epigenomic reorganization in the CNS, with potentially long-lasting effects on the transcription of the target gene. The *Hdac2* ASOs achieve this knockdown by blocking RNA Pol II elongation. This transcriptional inactivation may partly explain the long-term effects of a single application of ASO. Peptide nucleic acids (PNAs) that base pair with DNA, but have a peptide backbone, have been designed to target gene promoters and prevent RNA Pol II transcription through steric hindrance of transcription factor binding [36]. Our data demonstrate that ASOs also act on transcription even if they are designed to target sequences far downstream of the promoter. It will be of interest to discriminate whether ASOs act like PNAs in blocking the binding of transcriptional regulators, or if their effect of blocking transcription is initiated by turning over regulatory RNAs such as ecRNAs.

We are now adding the mechanism of directly blocking transcription to the handful of mechanisms ASOs employ to modulate RNA [37]. ASOs elicit mRNA reduction that is potent and long lasting without altering the underlying sequence, so they may be more attractive than some other gene therapy approaches, like CRISPR [38], in certain contexts. This is because the changes induced by ASOs are extremely specific and enduring, but not permanent or damaging to genomic sequences.

Altered HDAC2 protein levels lead to changes in the expression of other genes implicated in memory formation. In particular, we see changes in expression of genes associated with ERK signaling and immune functions in the hippocampus and cortex. ERK proteins have important roles in learning and memory, and are necessary for long-term potentiation of synaptic activity [39]. Additionally, we saw alterations in genes first identified as performing immune functions in peripheral tissues also promote cognition [40,41] and regulation of synaptic plasticity [42-45]. Examples of immune-related factors with

connections to memory we see in our datasets include Down syndrome cell adhesion molecule (DSCAM) proteins, pentraxins, tumor necrosis factor alpha, the complement system, and MHCII. Previous work shows that *Hdac2* regulates neuronal morphology [6], and we identified genes involved with cell adhesion and synapse formation in the cortex. We also found a subgroup of genes involved in flavonoid regulation in the hippocampus affected by *Hdac2* ASO1 treatment. Flavonoids are now being studied with regards to their role in cognitive enhancement and regulation of inflammation [46].

MATERIALS AND METHODS

ASOs

Hdac2-ASO1 (5′-CToCoAoCTTTTCGAGGTToCoCTA-3′), *Hdac2*-ASO2 (5′-AToGoCoA GTTTGAAGTCToGoGTC-3′), and non-targeting scrambled (SCR) ASO (5′-GToToToTCAAATACACCToToCAT-3′) were generated by IONIS using the phosphorothioate and 2′-MOE modified ASO platform. *Fos* ASOs (*Fos* mRNA ASO (5'-UCUGUCAGCTCCCTCCUCCG-3'), *Fos* ecRNA ASO1 (5'-AGAUUGGCTGCTTGGUGGGU-3'), *Fos* ecRNA ASO2 (5'-ACUAGCGTGTCCTCTGAGUGA-3'), and non-targeting SCR ASO (5'-GUUUUCAAATACACCUUCAU-3')) were ordered from IDT. Sequences are designed for targeting mouse transcripts. Underlined residues are deoxynucleosides, and all others are 2´-*O*-methoxyethyl (2'-MOE) nucleosides. All linkages are phosphorothioate except those indicated by "o" between residues, which are phosphodiester.

Cell culture

Primary cortical neuron cultures were made from P0 mice. Dissected cortices were treated with papain supplemented with cysteine, and triturated to dissociate neurons. Cells were passed through a 70 µm filter (Falcon), and grown in neurobasal complete media (neurobasal with 1x B27 supplement, 1mM sodium pyruvate, 1mM HEPES, 100U/mL penicillin, 100µg/mL streptomycin, and 0.5mM L-glutamine). Cells were treated overnight with FdU to kill dividing cells on day in vitro (DIV) 3, and 10µM ASO was

applied on DIV 5. For washout experiments, neurons were treated 2 days with 10μM ASO. Cells were rinsed with complete neurobasal media, left a few minutes, and media was replaced again. ½ media changes were done every 2 to 3 days for all primary culture experiments. New media for changes did not contain ASO.

Neuro2a (N2a) cells were obtained from ATCC and grown according to recommended conditions. For long treatments plates were coated in poly-L-lysine. Cells attached overnight, and media was changed to differentiation media (DMEM with L-glutamine without glucose, 10mM galactose, 100U/mL penicillin, 100μg/mL streptomycin, and 1x N2 supplement) to make differentiated N2a (dN2a). After 4 days, half the media was changed and supplemented with complete neurobasal media at a ratio of 1:400 neurobasal to differentiation media. Half media changes were done as needed. Replacement media contained drug at the same concentration as the initial treatment.

For *Fos* ecRNA experiments, N2a were transfected with GenMute reagent according the manufacturer's specifications with ASO at a final concentration of 60nM. Media was changed to differentiation media 5 hours after transfection, and 2 days later changed to neurobasal media. RNA was extracted the following morning.

Mice

Male B6129S F1 hybrid mice at 2 months of age were acquired from The Jackson Laboratory. All procedures were performed with Institutional Animal Care and Use Committee (IACUC)-approved protocols and conducted in full compliance with the Association for Assessment and Accreditation of Laboratory Animal Care (AAALAC).

In vivo ASO administration

ASOs were injected by unilateral ICV bolus injection of 300 μg. Mice were anaesthetized with 2% isoflurane and secured in a stereotaxic frame (David Kopf Instruments). ASOs were diluted to 60 μg/μl in saline and injected 15 mg/kg into the lateral ventricle (anterior/posterior [A/P], −0.2;

medial/lateral [M/L], −1.0; dorsal/ventral [D/V], −2.4 to the bregma) of 2-month-old mice at a rate of 1 µl/min. After the injection, the needle was kept in place for 5 min., followed by suturing of the incision. Intravenous (IV) injections of ASO (300 µg) were done into the tail vein. 3 animals per group per time point were treated.

Targeted gene expression analysis

For mouse tissue samples, total RNA and DNA was extracted with AllPrep® DNA/RNA/miRNA kit (Qiagen). RNA was extracted from the right hemisphere of the brain. Total mRNA was reverse transcribed using the iScript cDNA Synthesis Kit (Bio-Rad). For culture samples the RNeasy plus kit (QIAGEN) and SuperScript VILO (Invitrogen) was used according to manufacturer's instructions. qPCR was performed with the CFX96 Optical Reaction Module (Bio-Rad) using SYBR green (Bio-Rad). Relative gene expression from in vivo samples was determined using the ΔΔCt method [47] and normalized to a housekeeping gene. qPCR primer sequences are listed in Table S1.

Western blots

Tissue from the left hemisphere of the brain was homogenized in RIPA buffer. Protein samples were run on 4-20% TGX Gels (Bio-Rad) and then transferred to PVDF membranes (Millipore) using standard protocols. Primary antibodies were: HDAC2 (Abcam ab12169) and actin (Abcam ab3280). Secondary antibodies were goat anti mouse IR 680 (LiCor #926-68020) and goat anti mouse IR 800 (LiCor #926-32210). Membranes were imaged on the LiCor Odyssey fluorescence imaging system.

Object location memory test (OLM)

Mice were habituated to an opaque polyurethane open box (10 × 10 × 12 in. (x, y, z)) containing autoclaved bedding with one black line spatial cue for 3 days (5 min. per day) prior to training. Mice were trained for 10 min. with two 50 ml beakers in a particular location. 24 hr. after training, one beaker

was moved to a novel location and the mice were tested for 5 min. Videos were scored by hand and blinded to subject identity. Object interaction was scored as previously described [48].

Chromatin immunoprecipitation (ChIP)

RNA Pol II ChIP cells were cross-linked with 0.5% formaldehyde in neurobasal for 10 minutes at RT. The crosslinking was stopped with glycine, and cells were immediately placed on ice and lysed in L1 buffer. Purification of chromatin was done as previously described [31]. Chromatin was sonicated in Diagenode mini water bath to 100-400 bp fragments. 5µg of antibody 3E8, 50µL of protein G coated dynabeads, and 68µg of chromatin were used per IP. Signal from Intron 1 primers was standardized to input, normalizing to *Gapdh* intron primers. Fold change was calculated relative to SCR ASO signal from *Hdac2* exon 5 primer from each batch of chromatin. ½ of the plates were treated with SCR ASO and *Hdac2* ASO1 for each preparation, so batch effects could be taken into account.

For DNMT3a ChIP, cells were trypsinized and washed in 1x PBS. Pelleted cells were resuspended in 1x PBS and cross-linked with 2mM freshly dissolved disuccinimidyl glutarate for 45 min. and 1% formaldehyde for the last 15 min. at 4°C with shaking. Pull down was done with 15µL total of a 1:1 mix of Protein A and Protein G dynabeads and 1.5µg of antibody (Abcam ab2850). 50-75µg chromatin was used per pull down.

Methyl-DNA immunoprecipitation (MeDIP)

DNA was isolated with DNeasy blood and tissue kit (QIAGEN) and sonicated to 300-1000bp with a Diagenode bioruptor for 10-16 rounds of 15s on 90s off at a concentration of 20ng/µL in 300µL volume. 3-5µg DNA, 30µL prewashed protein G dynabeads, and 10µg EpiGentek OptimAb 5-Methylcytosine (33D3) monoclonal antibody were used per pull-down. Pull down was done in IP buffer (5mg/mL BSA and 0.05% Triton X-100 in 1x PBS) at 4 °C for 2 hours with rotation. Beads were washed three times with IP buffer on a magnetic stand. DNA was dissociated from beads with 1mg/mL proteinase K

overnight at 50°C with shaking, extracted with phenol/chloroform, precipitated in NaCl and ethanol, washed in 70% ethanol, and resuspended in TE buffer.

Nuclear run-on (NRO)

This procedure is based on several sources [30,31,49,50] and optimized to reduce non-specific RNA binding. Nuclei were extracted as previously described [31], with lysis buffer containing Igepal concentration optimized based on cell type - 0.25% for dN2a and 0.5% for primary neurons. The run-on reaction was done as previously described [31]. RNA concentration was measured by nanodrop and normalized. 30µL Protein G dynabeads were washed twice in BrU binding buffer, rotated at RT with 2µg Anti-BrdU antibody (Santa Cruz Biotech, IIB5, sc-32323) in BrU binding buffer for 10 min., blocking buffer was added, and beads rotated another 30 min. at RT. After blocking, beads were washed 2 times with binding buffer. The blocked bead mixture was combined with RNA sample, and put on a rotating stand for 30 min. at RT. After binding, beads were washed twice for 2 min. in BrU binding buffer, once in low salt buffer, once in high salt buffer and twice in TET buffer. Buffer compositions were previously published [50]. On the final TET wash, beads were moved to a new tube, TET was removed, and TRIzol was used to elute and purify RNA as previously described [49]. Three rounds of immunoprecipitation were conducted on each sample. Purified RNA samples were heated at 65°C for 5 min. then placed on ice at least for 2 min. prior to IP or reverse transcription reaction. Multiscribe reverse transcriptase was used to make cDNA according to manufacturer's recommendations.

For the non-specific binding check, NRO samples made with UTP were run in parallel to samples made with BrUTP. The elution after the third round of BrdU immunoprecipitation was run on a bioanalyzer Eukaryote Total RNA Pico Series II chip according the manufacturer's instructions. Signal intensity is normalized across all samples in the gel-like output image.

Total RNA-seq

Total RNA-seq libraries were prepared using the TruSeq Stranded Total RNA Library Prep Kit with Ribo-Zero Gold (Illumina) according to manufacturer's instructions. 1µg of RNA was used as starting material and amplified with 12 PCR cycles. Library size distribution was checked with an Agilent 2100 Bioanalyzer and quantity was determined using qPCR. Libraries were sequenced on an Illumina HiSeq 2500 using a 50-cycle rapid run kit or an Illumina NextSeq instrument using a 75-cycle high throughput kit. Reads were aligned to the GRCm38.p3 mouse genome and transcriptome using TopHat [51] and differential expression tests were performed using featureCounts [52] and edgeR [53,54] with standard settings. DAVID [55,56] was used for functional annotation of genes. Heatmaps were generated with gplots package in R.

Statistics

ANOVA and Student's *t* tests were conducted in GraphPad Prism version 8 with indicated post-hoc tests.

FUNDING AND DISCLOSURE

These studies were supported by grants from the NIH (MH091122 and MH57014 to J.D.S., and T32 MH065215 to C.B.G.), the Defense Advanced Research Projects Agency (HR0011-16- C-0065, HR0011-14-1-0001, HR0011-12-1-0015, and FA8650-13-C-7340), and start-up funds from Vanderbilt University. The views, opinions and/or findings contained in this article are those of the authors and should not be interpreted as representing the official views or policies of the Department of Defense or the U.S. Government. Distribution Statement "A" (Approved for Public Release, Distribution Unlimited).

S.T.M., S.G.P. and T.P.M. were Abbott Laboratories employees when these experiments were conducted. H.B.K., H.Z., D.J.E., and E.E.S. are or were employees of IONIS Pharmaceuticals. The remaining authors have nothing to disclose.

ACKNOWLEDGEMENTS

We would like to thank Tim Broderick and Bruce Howard for many helpful discussions over the course of this project. The authors sincerely appreciate help from Jane Wright, Garrett Kaas, and Joseph Weiss with primary neuron generation and isolation, and help from Colin Fricker with qPCR. We thank Benjamin Coleman and Joseph Weiss for their efforts in preliminary data generation.

AUTHOR CONTRIBUTIONS

C.B.G., S.G.P., K.A.G., A.J.K., T.P.M., S.T.M. aided with experimental design and analysis. S.G.P. conducted sequencing prep and bioinformatics. C.B.G. conducted in vitro assays and analysis of RNA-seq data. K.A.G. was project manager for Vanderbilt's team, and conducted the tail vein injection experiments. A.J.K. did ICV infusions. A.J.K and R.L.M. aided with expression analysis, animal behavior, and colony maintenance. R.L.M. conducted immunoblotting. H.B.K. and E.E.S. designed and developed the *Hdac2*-targeting ASOs. S.B.G. redesigned and conducted experiments with the mouse *Fos* ASOs. C.B.G., S.G.P., T.P.M., and J.D.S wrote the manuscript with assistance from all authors.

ADDIONAL INFORMATION

Data and materials availability: Sequencing data has been deposited in Gene Expression Omnibus (GEO) with the accession number GSE124726. All relevant data from this study are available on request from the corresponding authors (J.D.S. or T.P.M.).

Supplementary Materials:

Within supplemental document (Table S1. qPCR primer sequences, Fig. S1. ASO specificity in another cell culture system, Fig. S2. Expression of *Hdac2* RNA across the gene and in different tissues with different administration strategies, Fig. S3. Effect of ASOs on ecRNA and DNA methylation, Fig. S4. Reduced transcriptional elongation at *Hdac2* after *Hdac2* ASO treatments in dN2a, HDAC inhibitors do not affect *Hdac2* transcription, and FLAVO represses *Hdac2* in dN2a).

Separate excel files contain fold changes and cluster assignment for genes in Fig. 3.:

Table S2. Significantly changed genes at learning time points in cortex.

Table S3. Significantly changed genes at learning time points in hippocampus.

REFERENCES

1 Alarcon JM, Malleret G, Touzani K, Vronskaya S, Ishii S, Kandel ER, et al. Chromatin acetylation, memory, and LTP are impaired in CBP+/- mice: a model for the cognitive deficit in Rubinstein-Taybi syndrome and its amelioration. Neuron. 2004;42(6):947-59.

2 Korzus E, Rosenfeld MG, Mayford M. CBP histone acetyltransferase activity is a critical component of memory consolidation. Neuron. 2004;42(6):961-72.

3 Wood MA, Kaplan MP, Park A, Blanchard EJ, Oliveira AM, Lombardi TL, et al. Transgenic mice expressing a truncated form of CREB-binding protein (CBP) exhibit deficits in hippocampal synaptic plasticity and memory storage. Learn Mem. 2005;12(2):111-9.

4 Levenson JM, O'Riordan KJ, Brown KD, Trinh MA, Molfese DL, Sweatt JD. Regulation of histone acetylation during memory formation in the hippocampus. J Biol Chem. 2004;279(39):40545-59.

5 Hawk JD, Florian C, Abel T. Post-training intrahippocampal inhibition of class I histone deacetylases enhances long-term object-location memory. Learn Mem. 2011;18(6):367-70.

6 Guan JS, Haggarty SJ, Giacometti E, Dannenberg JH, Joseph N, Gao J, et al. HDAC2 negatively regulates memory formation and synaptic plasticity. Nature. 2009;459(7243):55-60.

7 Kennedy AJ, Rahn EJ, Paulukaitis BS, Savell KE, Kordasiewicz HB, Wang J, et al. Tcf4 Regulates Synaptic Plasticity, DNA Methylation, and Memory Function. Cell Rep. 2016;16(10):2666-85.

8 Southwell AL, Skotte NH, Kordasiewicz HB, Ostergaard ME, Watt AT, Carroll JB, et al. In vivo evaluation of candidate allele-specific mutant huntingtin gene silencing antisense oligonucleotides. Mol Ther. 2014;22(12):2093-106.

9 Meng L, Ward AJ, Chun S, Bennett CF, Beaudet AL, Rigo F. Towards a therapy for Angelman syndrome by targeting a long non-coding RNA. Nature. 2015;518(7539):409-12.

10 Kordasiewicz HB, Stanek LM, Wancewicz EV, Mazur C, McAlonis MM, Pytel KA, et al. Sustained therapeutic reversal of Huntington's disease by transient repression of huntingtin synthesis. Neuron. 2012;74(6):1031-44.

11 Stein CA, Castanotto D. FDA-Approved Oligonucleotide Therapies in 2017. Mol Ther. 2017;25(5):1069-75.

12 Jensen MP, Barker RA. Disease-Modification in Huntington's Disease: Moving Away from a Single-Target Approach. J Huntingtons Dis. 2019.

13 Wu H, Lima WF, Zhang H, Fan A, Sun H, Crooke ST. Determination of the role of the human RNase H1 in the pharmacology of DNA-like antisense drugs. J Biol Chem. 2004;279(17):17181-9.

14 Alter J, Lou F, Rabinowitz A, Yin H, Rosenfeld J, Wilton SD, et al. Systemic delivery of morpholino oligonucleotide restores dystrophin expression bodywide and improves dystrophic pathology. Nat Med. 2006;12(2):175-7.

15 Sazani P, Gemignani F, Kang SH, Maier MA, Manoharan M, Persmark M, et al. Systemically delivered antisense oligomers upregulate gene expression in mouse tissues. Nat Biotechnol. 2002;20(12):1228-33.

16 Merkhofer EC, Hu P, Johnson TL. Introduction to cotranscriptional RNA splicing. Methods Mol Biol. 2014;1126:83-96.

17 Osheim YN, Miller OL, Jr., Beyer AL. RNP particles at splice junction sequences on Drosophila chorion transcripts. Cell. 1985;43(1):143-51.

18 Wu ZA, Murphy C, Callan HG, Gall JG. Small nuclear ribonucleoproteins and heterogeneous nuclear ribonucleoproteins in the amphibian germinal vesicle: loops, spheres, and snurposomes. J Cell Biol. 1991;113(3):465-83.
19 Beyer AL, Bouton AH, Miller OL, Jr. Correlation of hnRNP structure and nascent transcript cleavage. Cell. 1981;26(2 Pt 2):155-65.
20 El-Brolosy MA, Stainier DYR. Genetic compensation: A phenomenon in search of mechanisms. PLoS Genet. 2017;13(7):e1006780.
21 Wu HJ, Lima WF, Zhang H, Fan A, Sun H, Crooke ST. Determination of the role of the human RNase H1 in the pharmacology of DNA-like antisense drugs. The Journal of biological chemistry. 2004;279(17):17181-89.
22 Meng L, Ward AJ, Chun S, Bennett CF, Beaudet AL, Rigo F. Towards a therapy for Angelman syndrome by targeting a long non-coding RNA. Nature. 2015;518(7539):409-12.
23 Geary RS, Norris D, Yu R, Bennett CF. Pharmacokinetics, biodistribution and cell uptake of antisense oligonucleotides. Adv Drug Deliv Rev. 2015;87:46-51.
24 Cossum PA, Sasmor H, Dellinger D, Truong L, Cummins L, Owens SR, et al. Disposition of the 14C-labeled phosphorothioate oligonucleotide ISIS 2105 after intravenous administration to rats. J Pharmacol Exp Ther. 1993;267(3):1181-90.
25 Smith RA, Miller TM, Yamanaka K, Monia BP, Condon TP, Hung G, et al. Antisense oligonucleotide therapy for neurodegenerative disease. J Clin Invest. 2006;116(8):2290-6.
26 Savell KE, Gallus NV, Simon RC, Brown JA, Revanna JS, Osborn MK, et al. Extra-coding RNAs regulate neuronal DNA methylation dynamics. Nat Commun. 2016;7:12091.
27 Di Ruscio A, Ebralidze AK, Benoukraf T, Amabile G, Goff LA, Terragni J, et al. DNMT1-interacting RNAs block gene-specific DNA methylation. Nature. 2013;503(7476):371-6.
28 Kim TK, Hemberg M, Gray JM, Costa AM, Bear DM, Wu J, et al. Widespread transcription at neuronal activity-regulated enhancers. Nature. 2010;465(7295):182-7.
29 Hervouet E, Peixoto P, Delage-Mourroux R, Boyer-Guittaut M, Cartron PF. Specific or not specific recruitment of DNMTs for DNA methylation, an epigenetic dilemma. Clin Epigenetics. 2018;10:17.
30 Kim YJ, Greer CB, Cecchini KR, Harris LN, Tuck DP, Kim TH. HDAC inhibitors induce transcriptional repression of high copy number genes in breast cancer through elongation blockade. Oncogene. 2013;32(23):2828-35.
31 Greer CB, Tanaka Y, Kim YJ, Xie P, Zhang MQ, Park IH, et al. Histone Deacetylases Positively Regulate Transcription through the Elongation Machinery. Cell Rep. 2015;13(7):1444-55.
32 Zocchi L, Wu SC, Wu J, Hayama KL, Benavente CA. The cyclin-dependent kinase inhibitor flavopiridol (alvocidib) inhibits metastasis of human osteosarcoma cells. Oncotarget. 2018;9(34):23505-18.
33 Chao SH, Price DH. Flavopiridol inactivates P-TEFb and blocks most RNA polymerase II transcription in vivo. J Biol Chem. 2001;276(34):31793-9.
34 Phatnani HP, Greenleaf AL. Phosphorylation and functions of the RNA polymerase II CTD. Genes Dev. 2006;20(21):2922-36.
35 Komarnitsky P, Cho EJ, Buratowski S. Different phosphorylated forms of RNA polymerase II and associated mRNA processing factors during transcription. Genes Dev. 2000;14(19):2452-60.
36 Wang G, Xu XS. Peptide nucleic acid (PNA) binding-mediated gene regulation. Cell Res. 2004;14(2):111-6.
37 DeVos SL, Miller TM. Antisense oligonucleotides: treating neurodegeneration at the level of RNA. Neurotherapeutics. 2013;10(3):486-97.

38 Gaj T, Gersbach CA, Barbas CF, 3rd. ZFN, TALEN, and CRISPR/Cas-based methods for genome engineering. Trends Biotechnol. 2013;31(7):397-405.
39 Peng S, Zhang Y, Zhang J, Wang H, Ren B. ERK in learning and memory: a review of recent research. Int J Mol Sci. 2010;11(1):222-32.
40 Nelson PA, Sage JR, Wood SC, Davenport CM, Anagnostaras SG, Boulanger LM. MHC class I immune proteins are critical for hippocampus-dependent memory and gate NMDAR-dependent hippocampal long-term depression. Learn Mem. 2013;20(9):505-17.
41 Ru M, Liu H. Association between Y-Maze Acquisition Learning and Major Histocompatibility Complex Class II Polymorphisms in Mice. Biomed Res Int. 2018;2018:6381932.
42 Fuerst PG, Koizumi A, Masland RH, Burgess RW. Neurite arborization and mosaic spacing in the mouse retina require DSCAM. Nature. 2008;451(7177):470-4.
43 Golan H, Levav T, Mendelsohn A, Huleihel M. Involvement of tumor necrosis factor alpha in hippocampal development and function. Cereb Cortex. 2004;14(1):97-105.
44 O'Brien RJ, Xu D, Petralia RS, Steward O, Huganir RL, Worley P. Synaptic clustering of AMPA receptors by the extracellular immediate-early gene product Narp. Neuron. 1999;23(2):309-23.
45 Stevens B, Allen NJ, Vazquez LE, Howell GR, Christopherson KS, Nouri N, et al. The classical complement cascade mediates CNS synapse elimination. Cell. 2007;131(6):1164-78.
46 Bakoyiannis I, Daskalopoulou A, Pergialiotis V, Perrea D. Phytochemicals and cognitive health: Are flavonoids doing the trick? Biomed Pharmacother. 2019;109:1488-97.
47 Livak KJ, Schmittgen TD. Analysis of relative gene expression data using real-time quantitative PCR and the 2(-Delta Delta C(T)) Method. Methods. 2001;25(4):402-8.
48 Haettig J, Stefanko DP, Multani ML, Figueroa DX, McQuown SC, Wood MA. HDAC inhibition modulates hippocampus-dependent long-term memory for object location in a CBP-dependent manner. Learn Mem. 2011;18(2):71-9.
49 Roberts TC, Hart JR, Kaikkonen MU, Weinberg MS, Vogt PK, Morris KV. Quantification of nascent transcription by bromouridine immunocapture nuclear run-on RT-qPCR. Nat Protoc. 2015;10(8):1198-211.
50 Core LJ, Waterfall JJ, Lis JT. Nascent RNA sequencing reveals widespread pausing and divergent initiation at human promoters. Science. 2008;322(5909):1845-8.
51 Trapnell C, Pachter L, Salzberg SL. TopHat: discovering splice junctions with RNA-Seq. Bioinformatics. 2009;25(9):1105-11.
52 Liao Y, Smyth GK, Shi W. featureCounts: an efficient general purpose program for assigning sequence reads to genomic features. Bioinformatics. 2014;30(7):923-30.
53 Robinson MD, McCarthy DJ, Smyth GK. edgeR: a Bioconductor package for differential expression analysis of digital gene expression data. Bioinformatics. 2010;26(1):139-40.
54 McCarthy DJ, Chen Y, Smyth GK. Differential expression analysis of multifactor RNA-Seq experiments with respect to biological variation. Nucleic Acids Res. 2012;40(10):4288-97.
55 Huang da W, Sherman BT, Lempicki RA. Systematic and integrative analysis of large gene lists using DAVID bioinformatics resources. Nat Protoc. 2009;4(1):44-57.
56 Huang da W, Sherman BT, Lempicki RA. Bioinformatics enrichment tools: paths toward the comprehensive functional analysis of large gene lists. Nucleic Acids Res. 2009;37(1):1-13.

FIGURES

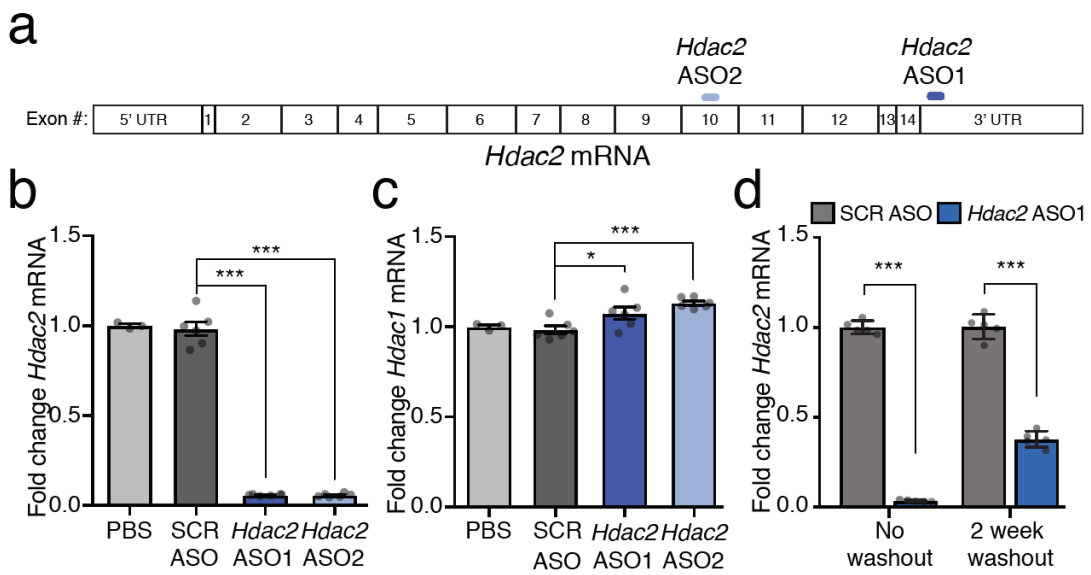

Fig. 1 Specificity of *Hdac2*-targeting ASOs. **a** Diagram of *Hdac2* mRNA with binding sites indicated for the ASOs used in this study. **b** Fold change in *Hdac2* mRNA expression after 1-week, 10 μM ASO treatment normalized to *Hprt* in mouse primary cortical neurons. **c** Same samples as used in panel B were tested with *Hdac1* specific primers. **d** Comparison of expression of *Hdac2* RNA after continuous 16-day treatment or 2-day treatment with ASO, cells were rinsed with media, media was replaced, and cells were incubated without ASO for two weeks with regular ½ media changes. Error bars represent ± standard error of the mean (SEM). Grey dots show relative expression values for individual replicates. *N* = 6 wells of cell culture from two biological replicates, each performed with 3 technical replicates. One-way ANOVA (**b** and **c**) with Dunnett's multiple comparisons *post hoc* test and two-way ANOVA with Sidak's multiple comparisons *post hoc* test (**d**) were used. * = $p < 0.05$, *** = $p < 0.001$.

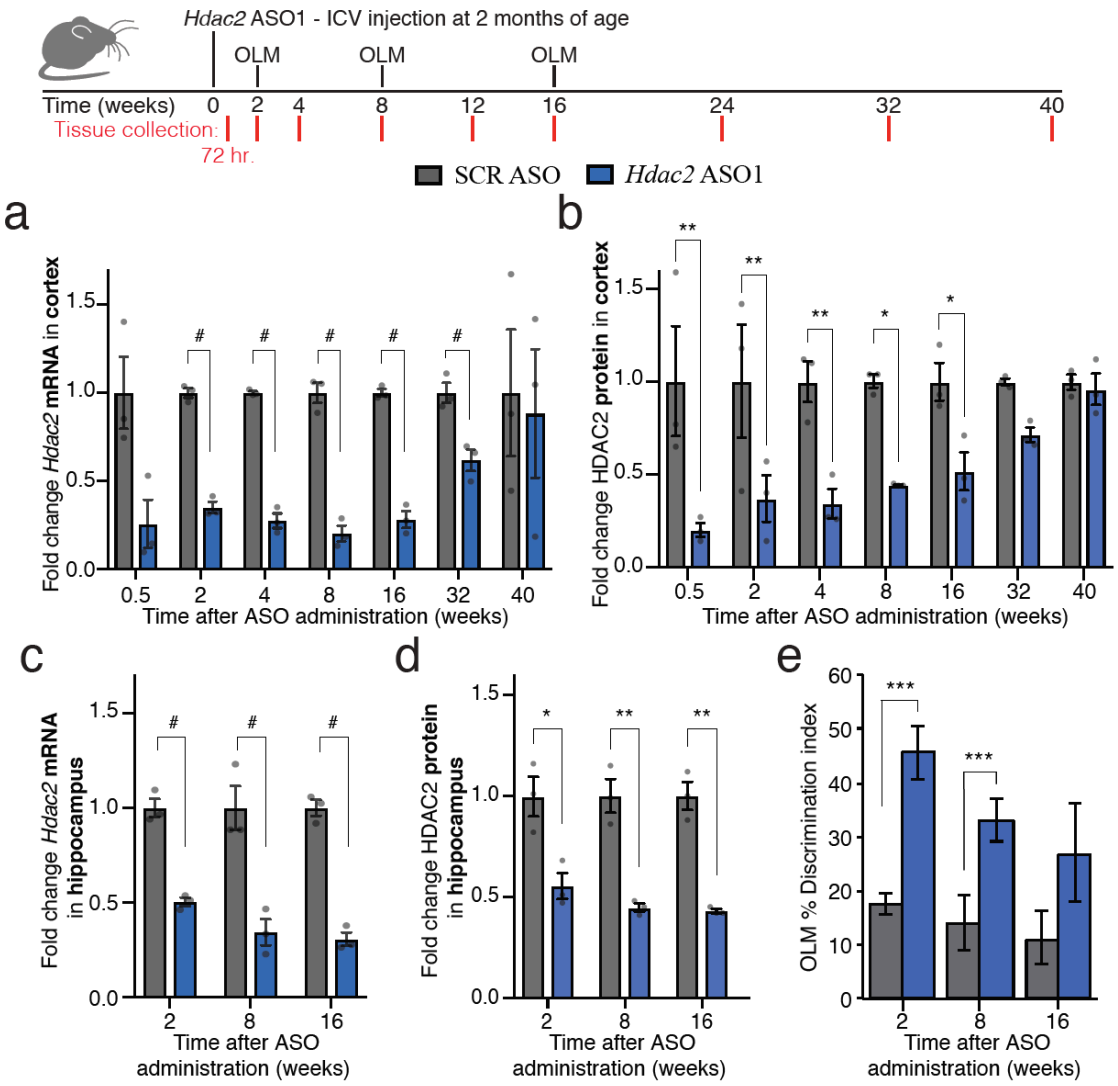

Fig. 2 *Hdac2* mRNA, HDAC2 protein, and cognitive enhancement levels across time after ICV injection of ASOs. **a** Fold change in *Hdac2* mRNA level for *Hdac2* ASO1 relative to SCR ASO group in RNA-seq of cortical samples. Relative expression change in *Hdac2* ASO1 group to SCR ASO was calculated from FPKM. **b** Quantitation of HDAC2 protein in *Hdac2* ASO1 group relative to SCR from western blots of cortical samples. **c** Fold change of *Hdac2* RNA in *Hdac2* ASO1 group relative to SCR in RNA-seq of hippocampal samples. **d** Quantitation of amount of HDAC2 protein in *Hdac2* ASO1 group relative to SCR from western blots in hippocampal samples. **e** Discrimination index of OLM test for *Hdac2* ASO1 and SCR ASO. *N* = 13, 12, 10, 12, 7, and 12 (for each bar left to right) animals. Error bars represent ± SEM. Grey dots show values for individual replicates. *N* = 3 animals for each time point. Two-way

ANOVA with Sidak's multiple comparisons *post hoc* test was conducted for western data. Mann-Whitney U test was done for OLM. # = FDR < 0.001. * = $p < 0.05$, ** = $p < 0.01$, *** = $p < 0.001$.

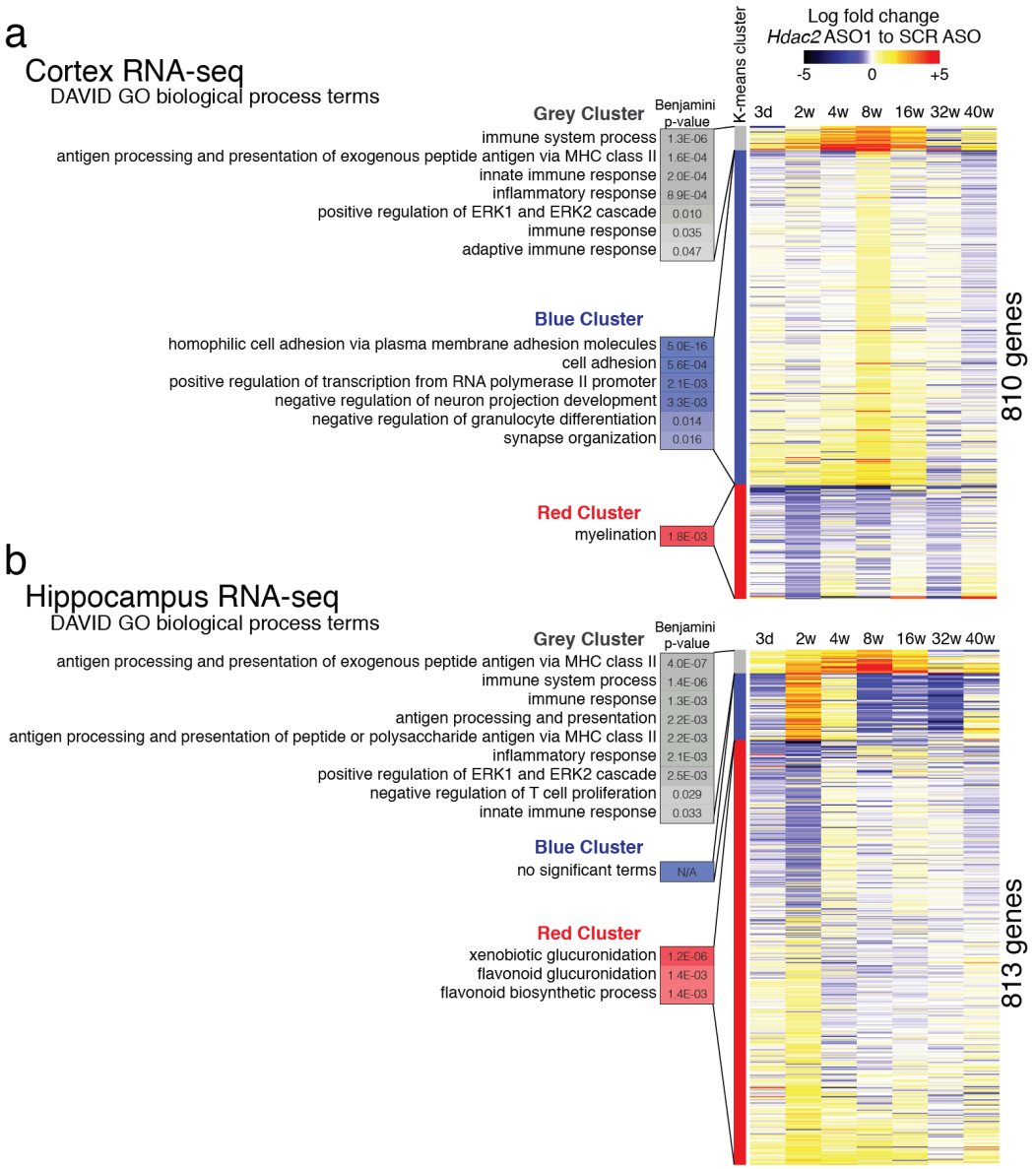

Fig. 3 Functions of significantly changed genes at memory enhancement timepoints – 2, 4, and 8 weeks. **a** Cortex RNA-seq and **b** Hippocampus RNA-seq. Three k-mean clusters utilizing fold changes across all timepoints for those genes with FDR < 0.1 some time between 2 and 8 weeks. In the heatmap, blue/black represents repression and orange/red represents activation. w = weeks, d = days. DAVID GO biological process terms are in the tables, and a Benjimini *p*-value < 0.05 was the cut off. This analysis was done for *N* = 3 animals for each time point.

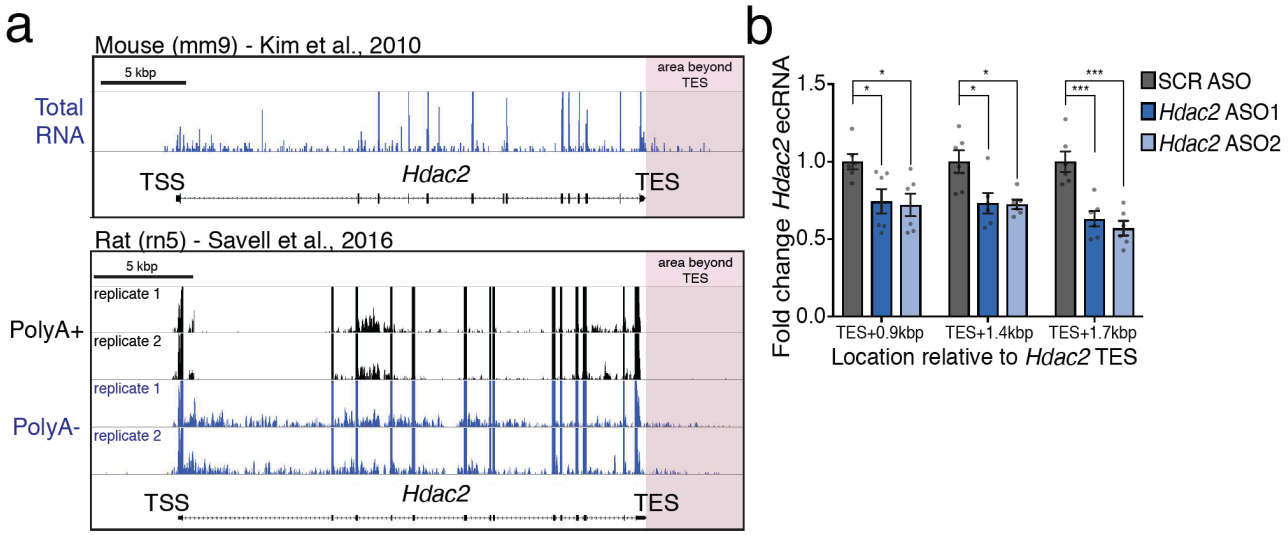

Fig. 4 *Hdac2* has a putative ecRNA and it is repressed by *Hdac2* ASOs. **a** RNA-seq reads at *Hdac2* gene from indicated sequencing libraries. Library reads were stranded, and only the reads representing sense transcripts relative to the direction of the *Hdac2* gene are shown (+ for mouse, - for rat). Gene tracks for rat were flipped to show the 5' end of *Hdac2* on the left. **b** Signal from RNA generated beyond the TES was detected with RT-qPCR using primers designed to the 3' end of the *Hdac2* ecRNA. Reverse transcription of RNA was done with random primers. N = 6 wells of cell culture from 2 biological replicates done in triplicate. All normalized to *Hprt*. Error bars represent ± SEM. Grey dots show values for individual replicates. Two-way ANOVA with Sidak's multiple comparisons *post hoc* test. * = $p < 0.05$, *** = $p < 0.001$.

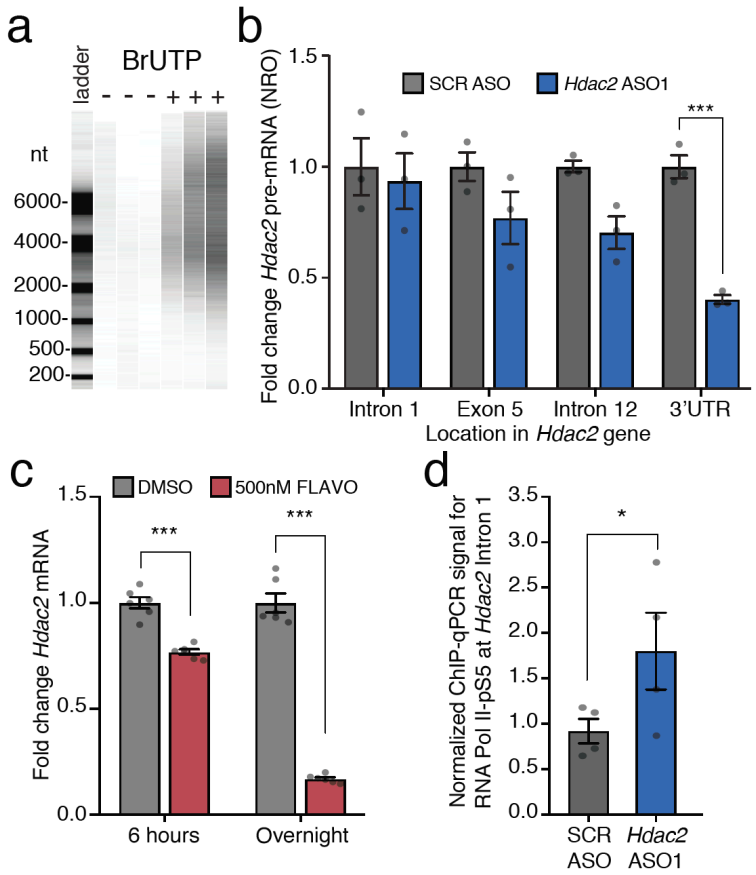

Fig. 5 Direct repression of *Hdac2* transcription by *Hdac2* ASO1. **a** Bioanalyzer high sensitivity RNA chip gel-like image of BrUTP immunoprecipitated NRO samples made with unlabeled UTP (-) or with BrUTP (+). Units for ladder are shown in nucleotides (nt). **b** RT-qPCR of NRO samples made from primary cortical neurons treated with ASOs. *N* = 3 biological replicates from independent preparations of primary neurons. **c** Primary cortical neurons were treated with FLAVO, and RNA was harvested after 6 hr. or after overnight incubation. *N* = 6 wells of cell culture from 2 biological replicates done in triplicate. **d** ChIP-qPCR with RNA Pol II pS5 antibody was conducted in primary neurons treated with SCR ASO and *Hdac2* ASO1. *N* = 4 biological replicates from independent preparations of primary neurons. Paired Students' *t* test. Two-way ANOVA with Sidak's multiple comparisons *post hoc* test was performed for panels **b** and **c**. Error bars represent ± SEM, grey dots show values for individual replicates. * = $p < 0.05$, *** = $p < 0.001$.